

UNCLASSIFIED

AD NUMBER
ADB292823
NEW LIMITATION CHANGE
TO Approved for public release, distribution unlimited
FROM Distribution authorized to U.S. Gov't. agencies only; Proprietary Info.; Jun 2003. Other requests shall be referred to U.S. Army Medical Research and Materiel Command, 504 Scott St., Ft. Detrick, MD 21702-5012.
AUTHORITY
USAMRMC ltr, 29 Jun 2004

THIS PAGE IS UNCLASSIFIED

AD _____

Award Number: DAMD17-01-1-0742

TITLE: A Model of Penetrating Traumatic Brain Injury
Using an Air Inflation Technique

PRINCIPAL INVESTIGATOR: Edward Moshang

CONTRACTING ORGANIZATION: EMTech Consultants, Incorporated
Baltimore, Maryland 21286

REPORT DATE: June 2003

TYPE OF REPORT: Final

PREPARED FOR: U.S. Army Medical Research and Materiel Command
Fort Detrick, Maryland 21702-5012

DISTRIBUTION STATEMENT: Distribution authorized to U.S. Government agencies only (proprietary information, Jun 03). Other requests for this document shall be referred to U.S. Army Medical Research and Materiel Command, 504 Scott Street, Fort Detrick, Maryland 21702-5012.

The views, opinions and/or findings contained in this report are those of the author(s) and should not be construed as an official Department of the Army position, policy or decision unless so designated by other documentation.

20031028 125

NOTICE

USING GOVERNMENT DRAWINGS, SPECIFICATIONS, OR OTHER DATA INCLUDED IN THIS DOCUMENT FOR ANY PURPOSE OTHER THAN GOVERNMENT PROCUREMENT DOES NOT IN ANY WAY OBLIGATE THE U.S. GOVERNMENT. THE FACT THAT THE GOVERNMENT FORMULATED OR SUPPLIED THE DRAWINGS, SPECIFICATIONS, OR OTHER DATA DOES NOT LICENSE THE HOLDER OR ANY OTHER PERSON OR CORPORATION; OR CONVEY ANY RIGHTS OR PERMISSION TO MANUFACTURE, USE, OR SELL ANY PATENTED INVENTION THAT MAY RELATE TO THEM.

LIMITED RIGHTS LEGEND

Award Number: DAMD17-01-1-0742

Organization: EMTech Consultants, Incorporated

Those portions of the technical data contained in this report marked as limited rights data shall not, without the written permission of the above contractor, be (a) released or disclosed outside the government, (b) used by the Government for manufacture or, in the case of computer software documentation, for preparing the same or similar computer software, or (c) used by a party other than the Government, except that the Government may release or disclose technical data to persons outside the Government, or permit the use of technical data by such persons, if (i) such release, disclosure, or use is necessary for emergency repair or overhaul or (ii) is a release or disclosure of technical data (other than detailed manufacturing or process data) to, or use of such data by, a foreign government that is in the interest of the Government and is required for evaluational or informational purposes, provided in either case that such release, disclosure or use is made subject to a prohibition that the person to whom the data is released or disclosed may not further use, release or disclose such data, and the contractor or subcontractor or subcontractor asserting the restriction is notified of such release, disclosure or use. This legend, together with the indications of the portions of this data which are subject to such limitations, shall be included on any reproduction hereof which includes any part of the portions subject to such limitations.

THIS TECHNICAL REPORT HAS BEEN REVIEWED AND IS APPROVED FOR PUBLICATION.

Frank Tortella

REPORT DOCUMENTATION PAGEForm Approved
OMB No. 074-0188

Public reporting burden for this collection of information is estimated to average 1 hour per response, including the time for reviewing instructions, searching existing data sources, gathering and maintaining the data needed, and completing and reviewing this collection of information. Send comments regarding this burden estimate or any other aspect of this collection of information, including suggestions for reducing this burden to Washington Headquarters Services, Directorate for Information Operations and Reports, 1215 Jefferson Davis Highway, Suite 1204, Arlington, VA 22202-4302, and to the Office of Management and Budget, Paperwork Reduction Project (0704-0188), Washington, DC 20503

1. AGENCY USE ONLY (Leave blank)		2. REPORT DATE June 2003	3. REPORT TYPE AND DATES COVERED Final (1 Jun 01 - 31 May 03)	
4. TITLE AND SUBTITLE A Model of Penetrating Traumatic Brain Injury Using an Air Inflation Technique			5. FUNDING NUMBERS DAMD17-01-1-0742	
6. AUTHOR(S) Edward Moshang Geoffrey Ling, M.D., Ph.D.				
7. PERFORMING ORGANIZATION NAME(S) AND ADDRESS(ES) EMTech Consultants, Incorporated Baltimore, Maryland 21286 E-Mail: emoshang@comcast.net			8. PERFORMING ORGANIZATION REPORT NUMBER	
9. SPONSORING / MONITORING AGENCY NAME(S) AND ADDRESS(ES) U.S. Army Medical Research and Materiel Command Fort Detrick, Maryland 21702-5012			10. SPONSORING / MONITORING AGENCY REPORT NUMBER	
11. SUPPLEMENTARY NOTES Original contains color plates: All DTIC reproductions will be in black and white.				
12a. DISTRIBUTION / AVAILABILITY STATEMENT Distribution authorized to U.S. Government agencies only (proprietary information, Jun 03). Other requests for this document shall be referred to U.S. Army Medical Research and Materiel Command, 504 Scott Street, Fort Detrick, Maryland 21702-5012.				12b. DISTRIBUTION CODE
13. ABSTRACT (Maximum 200 Words) This report describes a method for modeling penetrating traumatic brain injury (PTBI) caused by gunshot using rats as the subjects. The method will be an improvement over previously used techniques in that it is minimally invasive, humane and based on a mathematical approach that is founded on known ballistic biophysics. This technique specifically avoids using a fired projectile. The proposed use of this animal model should improve the understanding of the pathophysiology of penetrating traumatic brain injury.				
14. SUBJECT TERMS Math model for PTBI, ballistics biophysics, mechanical model, validation of models, penetrating wounds				15. NUMBER OF PAGES 25
				16. PRICE CODE
17. SECURITY CLASSIFICATION OF REPORT Unclassified	18. SECURITY CLASSIFICATION OF THIS PAGE Unclassified	19. SECURITY CLASSIFICATION OF ABSTRACT Unclassified	20. LIMITATION OF ABSTRACT Unlimited	

Table of Contents

Cover.....
SF298.....	2
Introduction.....	4
Construction of Mathematical Model.....	4
Description of Mechanical Device.....	11
In Vivo Studies.....	15
Key Research Accomplishments.....	25
Reportable Outcomes.....	25
Conclusions.....	28
References.....	29

Introduction

The objective of this study is to develop a method for modelling penetrating traumatic brain injury (PTBI) caused by gunshot using rats as the subjects. The method will be an improvement over previously used techniques in that it is minimally invasive, humane and based on a mathematical approach that is founded on known ballistic biophysics. This technique specifically avoids using a fired projectile. The proposed use of this animal model should improve the understanding of the pathophysiology of penetrating traumatic brain injury.

The initial objective is to develop a mathematical model for rats that describes the biophysics of wound formation following a ballistic injury. The bullet-size model will be the full metal jacket ammunition like the 7.62mm round and the 9mm which are most commonly used in the military. These equations can then be used generically to determine the dimensions of the salient features of ballistic injury, i.e. the size and shape of the permanent and temporary wound cavities, rapidity of expansion and duration of inflation.

The second objective is to develop a device for minimal invasive recreation of the wound in rats. This device will be based on an air inflation technique. It will be built exactly to precise specifications based on the above mathematical model. This device will be designed in accordance with all elements of the wound arising from a gunshot. The wound cavities assume the proper size, shape and for the appropriate duration.

The third objective will be to conduct in vivo validation study in rats to demonstrate that this model can recreate wounds similar to those caused by military gunshot. Histopathologic findings will be compared to the results from human gunshot victim autopsy reports and to the work of Carey et al (1989, 1990) using the now-abandoned fired projectile feline model.

This report contains the results of all of the above objectives.

Construction of the mathematical model

In the development of the mathematical model it is important to understand the flight characteristics of a projectile. The penetrating model consists of two distinct phases during its flight. These are the stable and the unstable phases of flight in a representative medium, like gelatin. The portion of a projectile's stable flight is a function of a number of variables, such as initial velocity, the shape of the projectile (drag characteristics), rotational velocity (spin stabilization) and the medium (μ) of travel. These are a few of the major parameters that come into play, and do not neglect the usual forces that act on the projectile such as gravity. Ammunition producers go through great pains to insure flight stability over very wide ranges of operation. Ballistic flight dynamics are well documented, Sellier and Kneubuehl's text (1994) as well as Bellamy and Zajtchuk's treatment in the Textbook of Military Medicine (chapter 4) both provide an excellent review of this subject. During stable flight energy transmitted (dissipated) into the medium is a minimum because the manufacturers have designed the projectile for maximally effective ranges and thereby minimizing the drag on the projectile. During unstable flight a maximal amount of energy is dissipated into its medium. This is the phase of flight we are focused on because it generates the large temporary cavity which causes the most damage. The key point underlying this study is that the center of pressure (CP) is not the same as the center of gravity (CG) of the projectile and as the projectile continues its path in the medium be it air, soap, gelatin or brain tissue it will eventually become unstable and tumble. The instability is due primary to drag forces on the projectile, along with the existence of a "yaw angle" (aerodynamically "angle of attack"). The combined effect of drag forces and small yaw angles eventually causes the CP to move, and in turn the projectile becomes unstable and tumbles.

During the tumbling action more energy will be dissipated into its surrounding medium. This will accentuate the production of a larger temporary cavity. The energy dissipated is modelled as an ellipsoid, where the major and minor axis governing its shape is related to the energy and associated velocity.

The model for describing the formation of the temporary cavity and its relation to the energy levels are described below, assuming the projectile remains intact after penetration. This assumption allows for the mass to remain a constant.

The energy available and amount of energy dissipate in its medium is characterized in figure 1.0, below where:

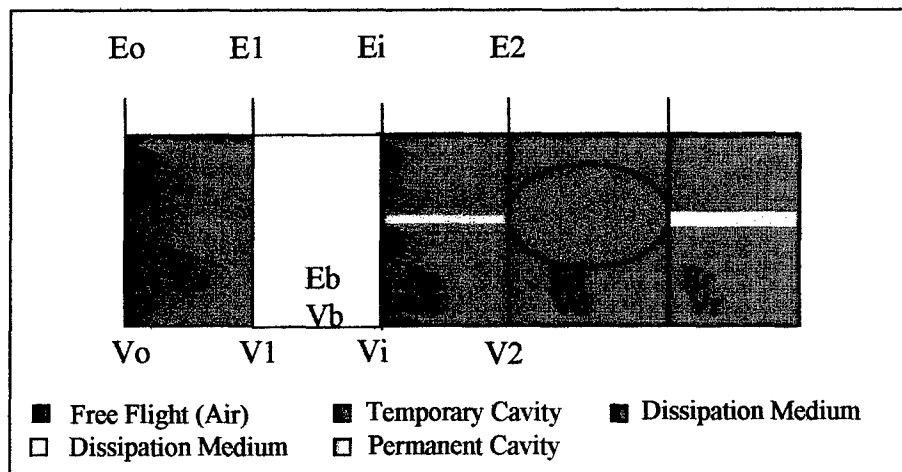


Figure 1.0 Energy Profile for Intact projectiles

- E_o is the muzzle energy, and V_o its associated muzzle velocity.
- E_a is the energy dissipated during free flight, which is a function of range to target and projectile design.
- E_1 is the energy available at impact, and V_1 is the associated velocity.
- E_b is energy dissipated on impact, and V_b the associated velocity.
- E_i is the initial impact energy available in the medium (μ) to form the temporary and permanent cavities.
- E_c is the energy dissipated in the medium (μ), while forming of the temporary cavity during its stable flight, and V_c is the associated velocity.
- E_2 is the energy available in the medium to form the large temporary cavity during the unstable flight, and V_2 is the associated velocity
- E_d is the energy dissipated in the medium (μ), while forming the temporary cavity during unstable flight or deformation of the projectile. V_d is the associated velocity.
- E_r is the residual energy, and V_r is the associated velocity.

The muzzle energy and velocities of all ammunition projectiles are well documented and have been shown to vary considerably. However for the purposes of this study a set of Firing Tables are provided in Sellier and Kneubuehl text (pages 356 to 373) and these data will be used as the basis of free flight performance (air). It measured data but represents typical manufactures' data. The projectiles under consideration are the 7.62 mm NATO round characterized by 9.5g

mass, muzzle velocity of 830 m/s and the 9mm parabellum round of 8g mass and muzzle velocity of 350 m/s. The 7.62 x39mm AK-47 round of 8 g mass and muzzle velocity of 716 m/s was also investigated. These were selected since they are very common military rounds and widely used in all arenas, including the 9mm for civilian law enforcement. The performance of 7.62mm NATO round will be representative of supersonic projectiles and the 9mm parabellum will represent the transonic or low velocity projectiles. Note that the muzzle velocity of the 9mm round is transonic but within 20 meters from the muzzle its velocity has dropped sufficiently so that upon impact it maybe considered subsonic.

The equations describing the energy and associated velocity are all related back to the muzzle energy (E_0) and muzzle velocity (V_0), with the fundamental assumption that the mass of the projectile is constant. The projectile may tumble after entering the brain or may deform (hollow point) but as long as the projectile does not fragment the mass will be constant. E_1 is the energy available at impact and V_1 is its associated velocity after a period of free flight. The velocity at impact (V_1) is derived by:

$$V_1 = V_0 - (Br) \times (\text{Range to Target from muzzle}) \quad (\text{equation 1.0})$$

where the constant (Br) is a derived constant, based on free flight data. This constant is a simple linear curve fit to manufacture's free flight data to permit ease of determining velocities at different ranges from the muzzle, but Br is different for each projectile because of the shape and construction of the projectile. Figure 1.2 illustrates the curves fit and Table 1.0 shows the error of the fit is less then 0.5% over the ranges of interest.

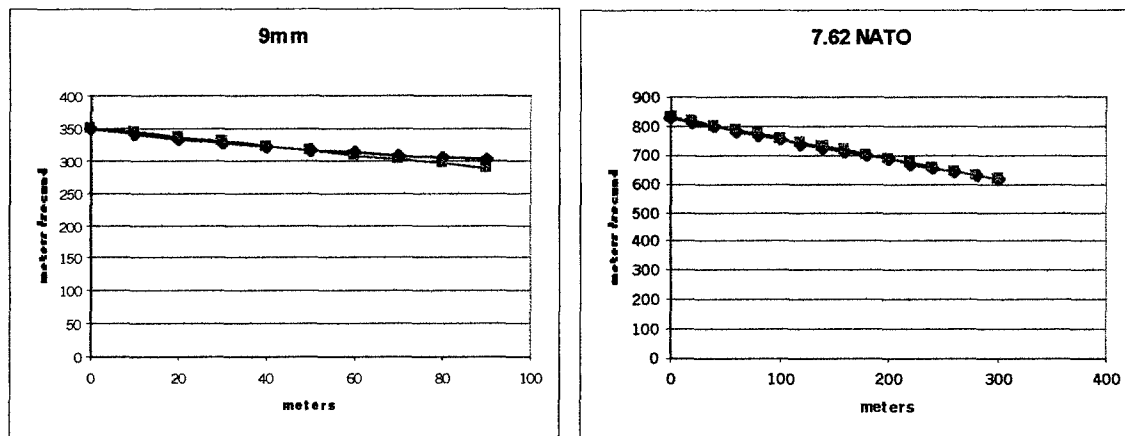


Figure 1.2 Extrapolated data for 9mm and 7.62 NATO Rounds

Range (Meters)	9mm Manufacture's Data (m/s)	9mm Extrapolated Data (m/s)	Range (Meters)	7.62mm Manufacture's Data (m/s)	7.62mm Extrapolated Data (m/s)
0	350	350	0	830	830
10	341	343	60	783	787
20	333	336	100	754	758
30	327	330	160	711	715
40	321	323	200	683	686
50	317	316	260	643	643
60	312	309	300	616	614

Table 1.0 Comparison of Extrapolated Data and Manufacture Data

It then follows that the available impact energy (E1) is:

$$E1 = (1/2) m V1^2 \quad (\text{equation 2.0})$$

where m is the mass of the projectile of interest and V1 is the result of equation 1.0, which depends on the range to target.

Since Ea is the energy dissipated during free flight, which is a function of range to target and projectile design, it follows;

$$Ea = Eo - E1. \quad (\text{equation 3.0})$$

Eb is energy dissipated on impact and depends on whether or not protective gear is used. Without protective gear, the penetration model developed by Sellier (ref a, pages 210-211) through the hair, scalp, skull, and into the brain changes the impact velocity by 110 m/s for the 9mm, or 48.4 joules of energy, which is approximately 10% of the available energy. Eb maybe represented as a percentage of E1 (the energy available at impact) and is computed as:

$$Eb = (X)E1, \quad (\text{equation 4.0})$$

where "X" is a number much less than 1.0, (0 < X < 1.0). However this parameter maybe modified if protective gear is used for the different types of projectiles. It follows that the associated magnitude of the velocity (Vb) is determined by:

$$Vb = (2Eb / m)^{1/2}. \quad (\text{equation 5.0})$$

Ei is the initial impact energy available in the medium (□) to form the temporary and permanent cavities and is derived as follows:

$$Ei = E1 - Eb, \text{ and} \quad (\text{equation 6.0})$$

$$Vi = (2Ei / m)^{1/2} \text{ its associated velocity.} \quad (\text{equation 7.0})$$

During the stable flight portion in the medium, equation (1) is modified to estimate the magnitude of the velocity just prior to the unstable flight. The modified equation simply accounts for the differences in densities between air and 20% gelatine and the difference is a factor of 848:1 changing equation (1) to:

$$V2 = Vi - Br (848)(D1), \quad (\text{equation 8.0})$$

where D1 is now the distance travelled in the medium prior to becoming unstable, which is observed for the gelatin tests.

The computed energy at this velocity (E2) is :

$$E2 = \frac{1}{2} m (V2)^2 \quad (\text{equation 9.0})$$

E2, and V2 now represent the available energy and associated velocity to form the larger temporary cavity as the projectile tumbles. From the data presented by Bellamy and Zajtchuk

(pages 130 – 131), projectiles typically dissipate 83% of the available energy in the formation of the larger temporary cavity when the flight becomes unstable.

Data also presented by Bellamy and Zajtchuk (page 134) also shows that there is a linear relationship between the maximum diameter of the temporary cavity and the impact velocity, similar to figure 1-3, below. This relationship shows the time to dissipate the available energy in the formation of the large temporary cavity is constant which is true if the medium is homogeneous like gelatin. Though the data shown by Bellamy and Zajtchuk is for soap, the behaviour in gelatin shows the same a linear relationship between maximum radius and velocity, but the specific time required to dissipate the energy is different. These results are from the mathematical model.

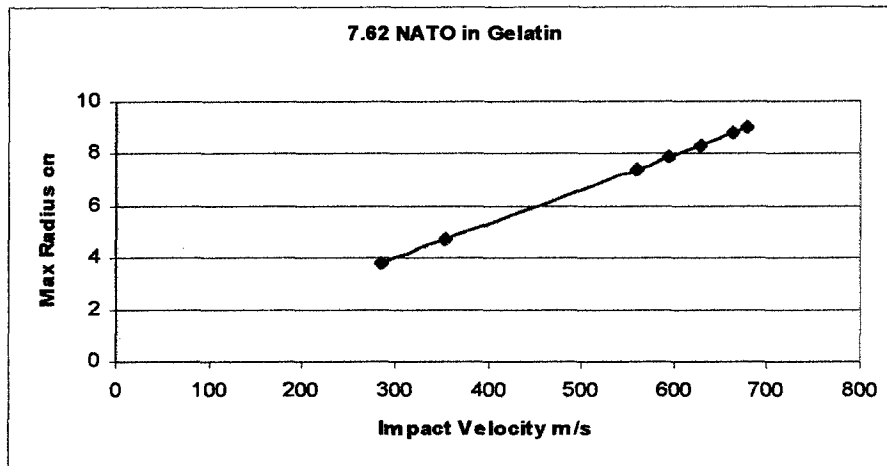


Figure 1-3 Maximum Radius vs. Velocity in Gelatin

Based on the gelatin data depicted below, figures 1-5 and 1-6, dynamic models are developed to depict the formation of the cavities after penetration. These data are obtained from U.S. Army Advanced Research Laboratories(ARL), in a series of reports by Bruchey et al (1979). Specifically, two models are required to capture the dynamics of the cavity formation. One represents the temporary cavity in stable flight after penetration and the other the large temporary cavity during the unstable flight. The size of the permanent cavity is strictly a function of the bullet selected. We have selected a typical 7.62 mm NATO round with a muzzle velocity of 830m/sec and muzzle energy of 3272 j. The 9mm characteristics are: muzzle velocity 350 m/sec; muzzle energy 490 j.

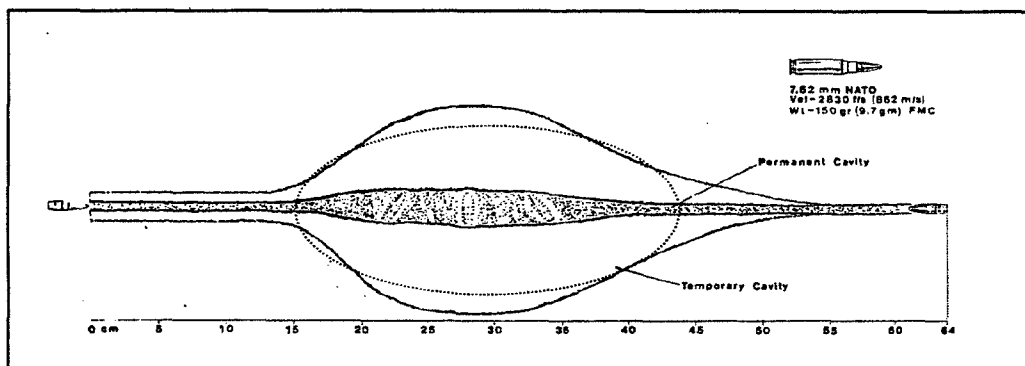


Figure 1-5 7.62 NATO in Gelatin

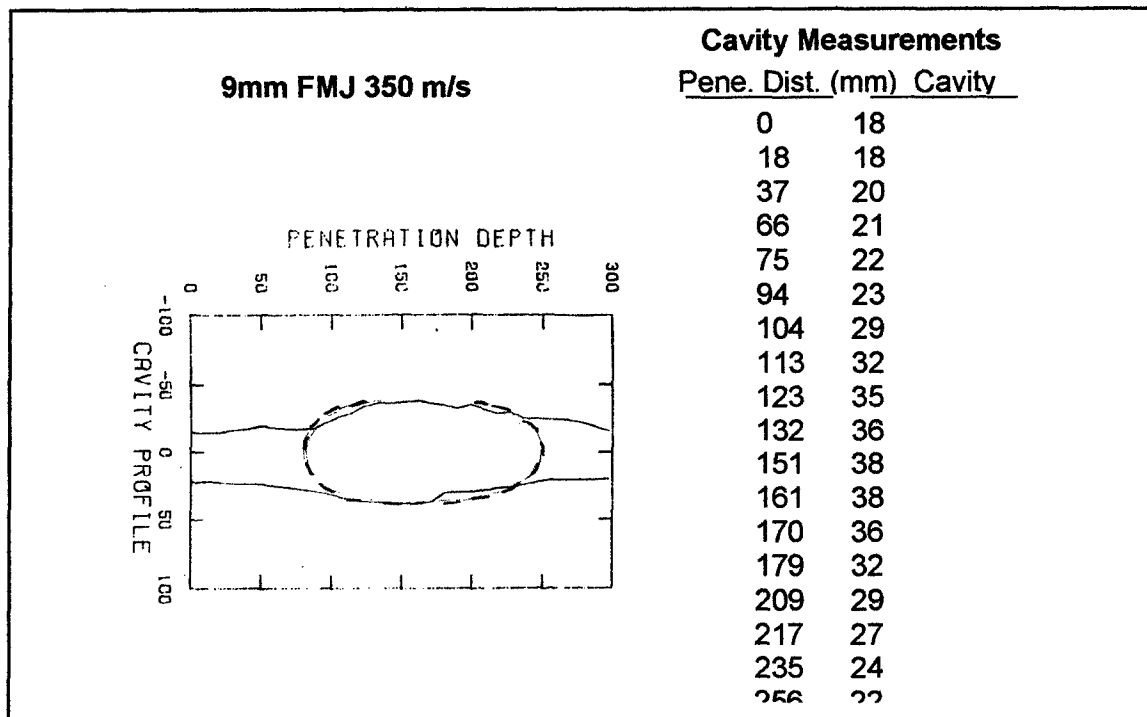


Figure 1-6 9mm in Gelatin

Dashed outline in both cases shows the large temporary cavity may be approximated by an ellipse, or in three dimensions an ellipsoid, except for different values associated with the major and minor axes of both rounds.

Figure 1-7 depicts the volumes of interest, Volume of the permanent cavity (V_p), the temporary cavity during stable flight (V_{ts}), and the temporary cavity due to unstable flight (V_t).

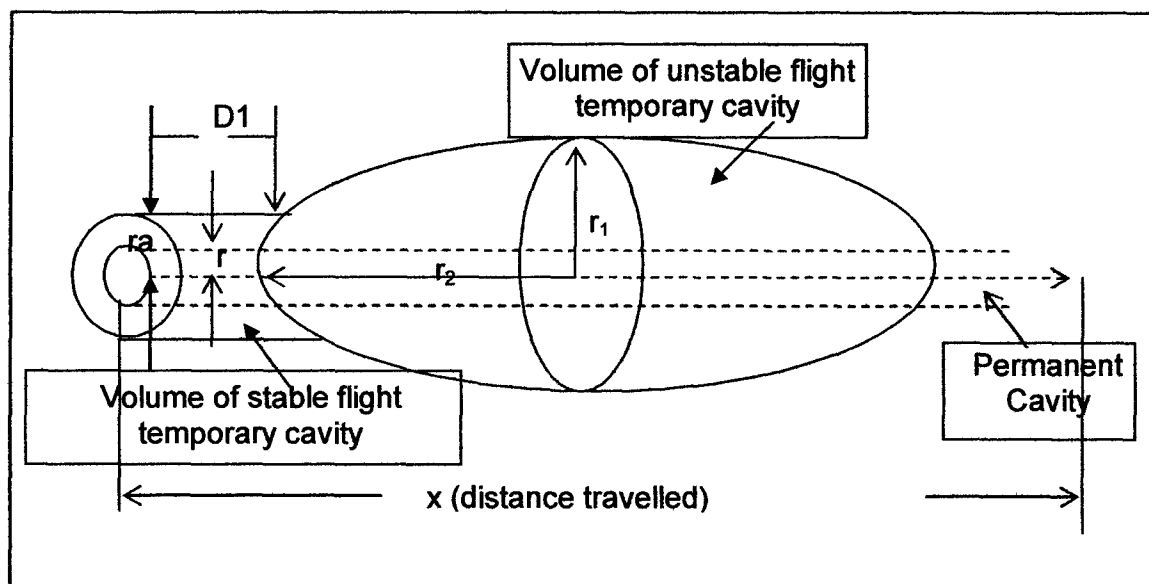


Figure 1-7 Geometric representations of the permanent and temporary volumes

Based on these observations, the calculations for energy and velocities as they relate to the geometric volumes are as follows:

The energy dissipated in forming the temporary cavity is (Ed),

$$E_d = K_3 * E_2. \quad (\text{equation 10})$$

and K3 is (0.83), representing factor for the dissipated energy.

The volume of the permanent cavity is expressed as:

$$V_p = \pi(r^2x), \quad (\text{equation 11})$$

where V_p is the volume of the permanent cavity, "r" is the radius of the projectile ($\frac{1}{2}$ its caliber) and "x" is the penetration distance t.

The volume of the temporary cavity during stable flight is expressed as:

$$V_{ts} = \pi(ra^2D1), \quad (\text{equation 12})$$

where V_{ts} is the volume of the cavity, "ra" is the cavity radius at penetration and D1 the penetration distance in the medium prior to going unstable.

The volume of the larger temporary cavity caused by the unstable flight is represented by:

$$V_t = (4\pi/3)r_2r_1^2, \quad (\text{equation 13})$$

where V_t is the volume of the temporary cavity, " r_2 " is the major radius of the temporary cavity and " r_1 " is the related minor axis where $r_1 = ka r_2$. The variables r_1, r_2 are related to velocity of the bullet within the cavity.

Both models equations (12) and (13) are combined to form the total dynamics of the temporary cavities. However it is noted that the amount of energy dissipated during stable flight is small in comparison to the energy dissipated unstable flight. The geometric representation of equation 13 is our main focus in the development of the mechanical model.

Since r_1, r_2 are related by, $r_1 = ka r_2$ and ka defines the shape of the ellipsoid. Based on the measured data of reference (c), ka for the 7.62 NATO round has a value of 0.61 and for the 9mm ka has a value of 0.43. Again, for different rounds there will be modifications to this parameter. It follows that r_1 and r_2 are related to the velocities; V_{t1} and V_{t2} , by:

$$r_1 = V_{t1}(TM) \text{ and } r_2 = V_{t2}(TM), \quad (\text{equations 14, 15})$$

where TM is the dissipation time during unstable flight and $V_d^2 = V_{t1}^2 + V_{t2}^2$.

After the formation of the large temporary cavity, the remaining energy is dissipated in the medium by continuing in flight or comes to rest. The residual energy is $E_r = E_2 - E_d$. E_r establishes whether on not sufficient energy remains to exit on the other side of the skull.

The combined volumes are the total volume of interest is represented by:

$$V_{\text{total}} = V_p + V_{\text{ts}} + V_t \quad (\text{equation 16})$$

However, of major interest is the large temporary cavity (V_t). This is the focus of our investigations. V_t is compared to the size of the human brain and then scaled down by 672.5:1 for the rat's brain size and designated as $V_{t \text{ rat}}$. The ratio of V_t to 1345 cm^3 is called the Reference Volume (V_{ref}); this number should be much less than one (1) for survival probabilities to increase. In cases where V_{ref} is equal to or greater than 1 (one), it simply means there is enough energy in forming the large temporary cavity to completely destroy the human brain. The value of 1345 cm^3 is representative of the volume of the human brain, as shown by Walker, A. and Shipman, P., 1996. The volume of the rat's brain is measure to be 2 cm^3 , which establishes the 672.5 to 1 ratio for scaling purposes. The scaling is required to establish the diameter of the probe to be inserted simulating the permanent cavity produced by the projectile.

Developing A Minimal Invasive Device

The device for the insertion into the rat's brain is a probe whose diameter is the scaled diameter of the bullet of interest (7.62mm). The probe contains air holes which are covered by Silex. When air is injected into the probe, by a pneumatic device, the Silex will expand and contract within 30 milliseconds simulating the expansion and contraction of the temporary cavity is produced by the unstable flight portion of the projectile. Figure 2.1 illustrates the design of the probe and Figure 2.2 is a representative prototype to use for the *in vivo* studies. Figure 2.3 shows the Pneumatic device producing the air.

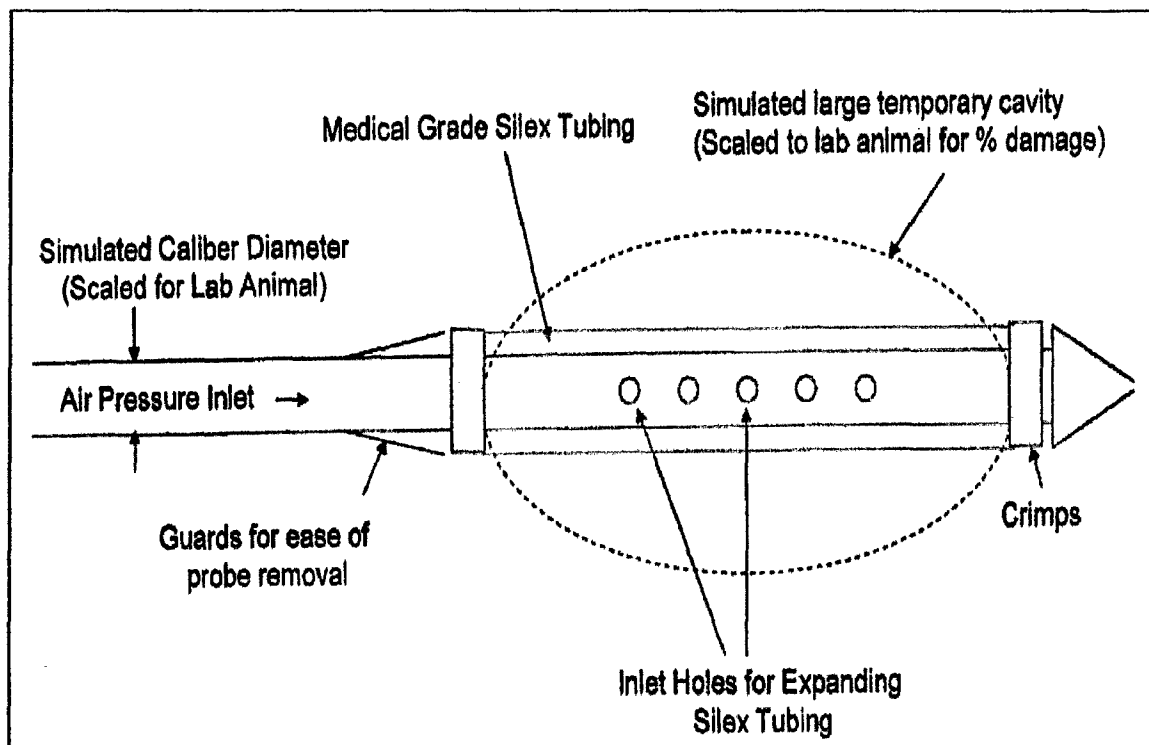


Figure 2.1 Illustrative Design of the Probe

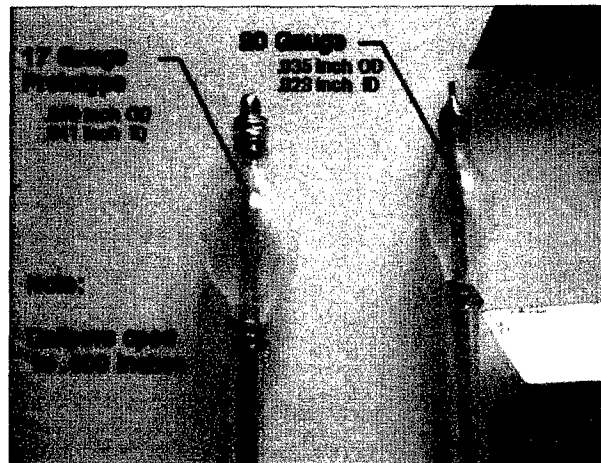
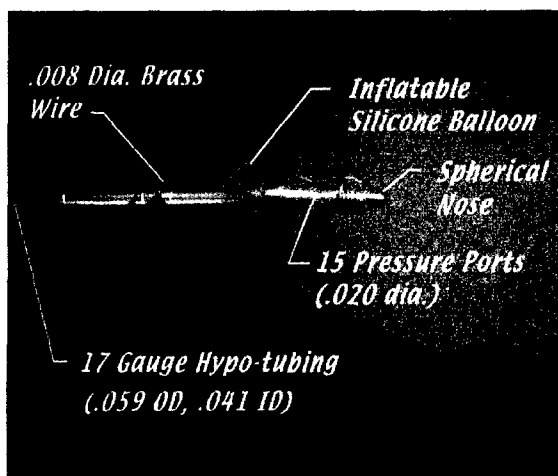


Figure 2.2 Prototype PTBI Probe (7.62mm for rat)

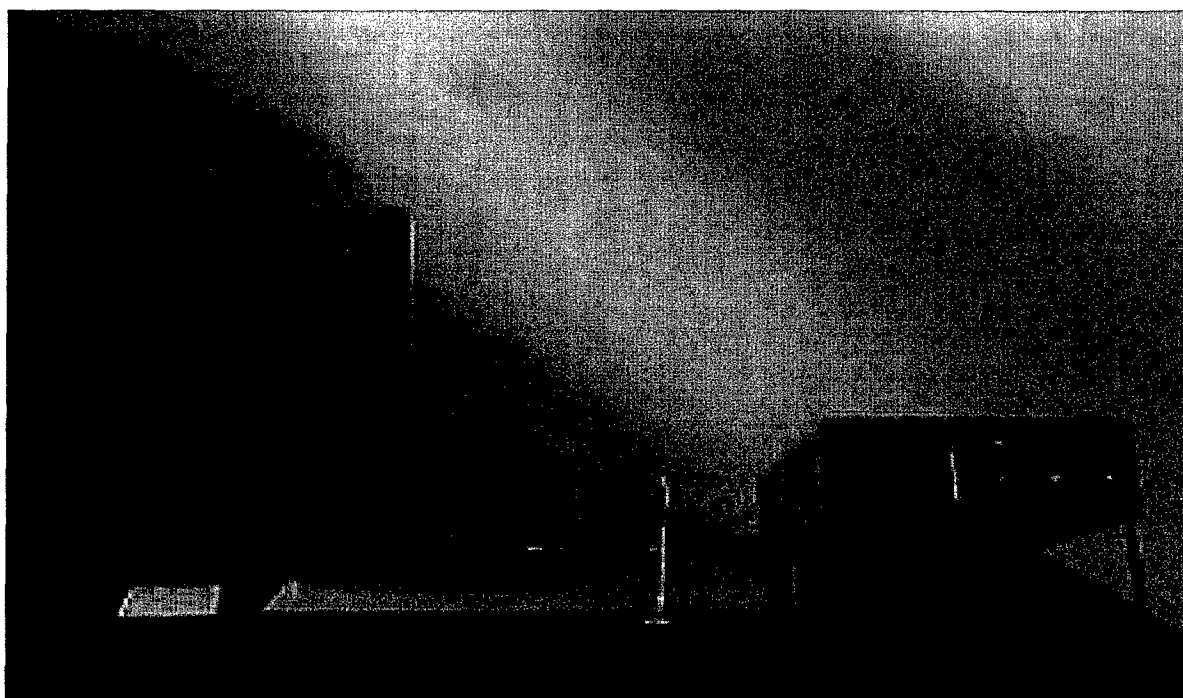


Figure 2.3 Pneumatic Device

The final probes for the 7.62 mm round, scaled for the rat are completed. The process for establishing the probe diameter which is representative of the projectile of interest starts with scaling the specific bullet (7.62 or 9mm) using the ratio of 672.5:1 (human brain volume to rat volume) to scale the size of the bullet down to the appropriate lab animal. The scaling assumes the actual bullet is a right circular cylinder and maintains the radius to length to be the same as shown in figure 2.4. Once the diameter is established, this defines the permanent cavity

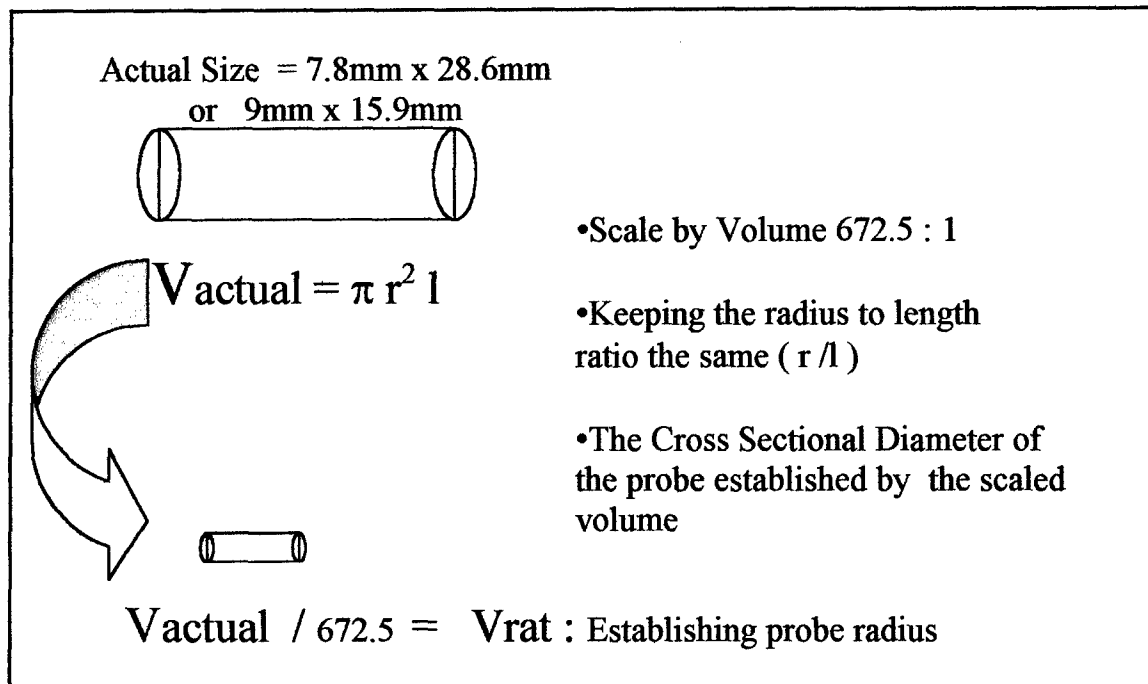


Figure 2.4 Process for scaling probe diameter

of the penetrating wound. The temporary cavity is generated by the expansion of the Silex balloon. The size (volume) of the balloon deployed depends on the amount of brain damage (energy dissipated into the temporary cavity). Since the rat's brain is 2cc in volume, the balloon deployment of 0.2cc represents a 10%, a 0.1 cc would be 5% and 0.3cc would be 15% damage. To simplify the implementation of the probe and balloon, the length of the ellipsoid representing the temporary cavity was held constant and the diameter was varied to meet the desired volume of damage. The following chart depicts the balloon diameters for a fixed length ellipsoid, for the different damage volumes.

Damage %	7.62 NATO	Volume (cm3)	9mm	Volume (cm3)	7.62 AK47	Volume (cm3)
	D(cm) L(cm)					
25	1.00 0.9525	0.501				
20	0.896 0.9525	0.400				
15	0.776 0.9525	0.301				
10	0.633 0.9525	0.201				
5	0.448 0.9525	0.101				

Since the length of the ellipsoid is held a constant, the balloon sizes for the different rounds would be the same for the same desired percentage damage. This represents a very slight change in the actual geometric shape of the ellipsoid. The reason for this decision was to avoid the necessity of changing probes for the same rounds when an increase (or decrease) in % damage is required. A probe change is always required for the different rounds because the permanent cavities are different.

The pneumatic device is a modified fluid percussion device. It was modified to be a closed air system which simply means when the correct amount of air is (statically) contained in the system,

each time an experiment is conducted the same amount of air remains and the results are repeatable. Figure 2.5 shows a block diagram of the system.

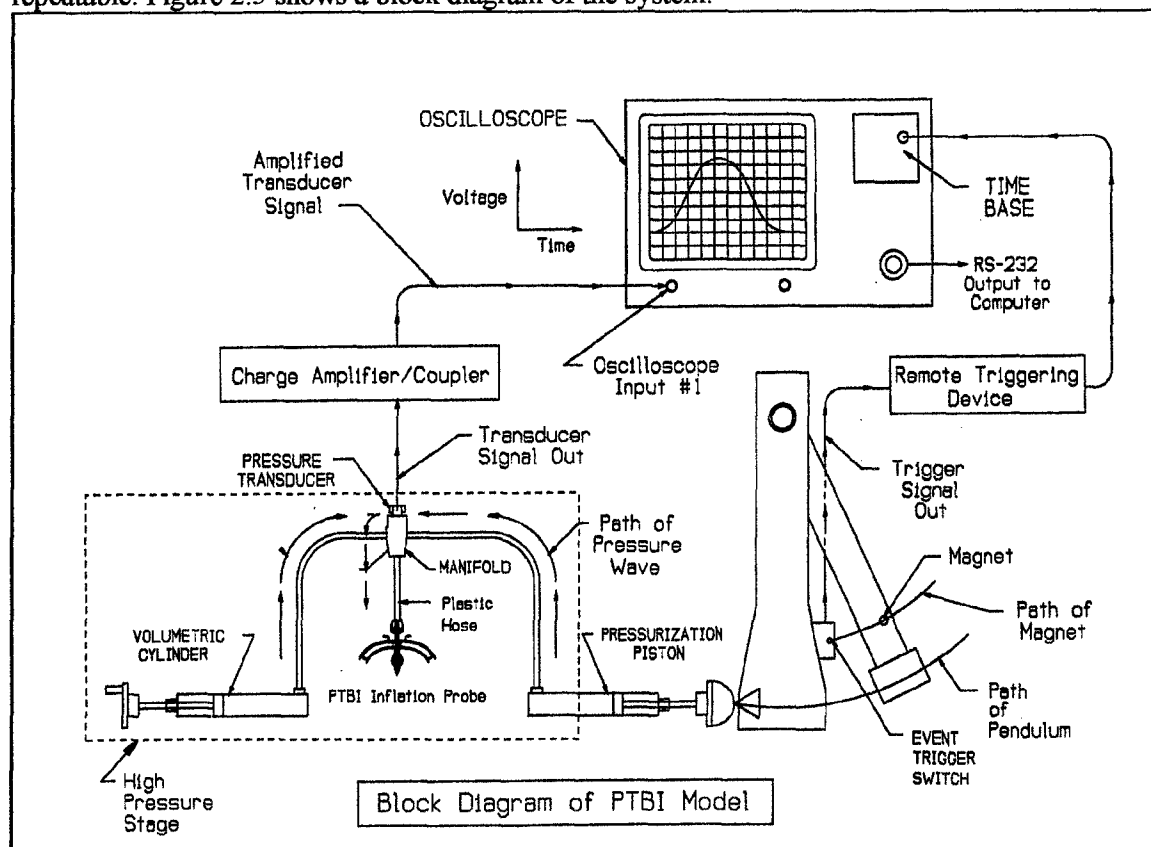


Figure 2.5 Block Diagram of the System.

The performance of the system is based on the weight of the pendulum, the volumetric cylinder and the pressure piston. These components determine the 2psi pressure and the 30msec. performance. With the pressure piston manually depressed, the volumetric cylinder is adjusted slowly for the proper (desired) balloon expansion. Releasing the piston after adjustment returns it to its ready (normal) position. The piston is then struck by the pendulum causing the balloon to expand, once struck the piston returns to its normal position, which brings about the balloon deflation. The entire operation from the time the piston is struck and its return to its normal position is 30 msec.

Since there were no devices in existence to delivery the pneumatic drive, our design performance data was derived from the existing fluid percussion devices. The 30 msec. response time does not reflect the expansion and collapse of the temporary cavity. We need to be down in the microsecond regime to replicate the actual expansion and collapse. However, it has yet to be proven that microsecond performance is required. At this point, further pathology should be conducted to establish design requirements on the mechanical model. The only immediate refinements to this model are to improve the packaging by deleting many of the flexible tubing and make solid connections. To try and improve on this mechanical model really needs a redesign.

The results from the invivo studies are summarized in the following paragraphs.

In Vivo Validation of the Prototype Air Inflation Model of Penetrating Brain Injury.

We have conducted a series of experiments on rats to determine the efficacy of the Air Inflation Model (AIM) of penetrating traumatic brain injury in modeling the human condition. Several parameters of brain injury were measured, including survival, behavioral outcome and pathology. The air inflation probe was inserted either occipital-frontally (O-F; back-to-front) or left-to-right, and inflated to produce either 0%, 5% or 10% damage to the brain, modeling after the different trajectories and damage produced by projectiles of varying size and velocities. Control animals were subjected to "sham" operations in which the probe was not inserted into the brain.

We had proposed originally to examine 5 different injury paths (i.e. back to front, side to side and oblique angles) as well as 3 different injury levels (i.e. 5%, 10% and 15% balloon); however, we experienced numerous quality assurance difficulties while refining the device. In particular, countless numbers of failed balloon deployments occurred during surgery, as well as balloons bursting upon deployment. Failures in balloon deployment amounted to the use of well over hundred rats. Since we can only assess deployment failures following behavioral and histological analysis of brain sections, this amounted to countless hours of lost time; hence, we could not complete all of the proposed trajectory paths and injury scales as originally proposed. However, once the probe was refined to its "final" form, we were able to examine the front-back and side-side injury paths with up to three AIM injury levels. From our results, we find that the front-back injury paradigm results in a greater loss of survival. As a rule of thumb, we adhered to the local IACUC's standard of lethality, in which a greater than 50% loss of survival be justified in the continuation of the procedure. The 15% injury level in the front-back lesions resulted in a 30% survival rate after only 7 surgeries. We felt that further experimentation to meet statistical requirement with a 30% survival rate was not justified, so we stopped further experimentation with the 15% balloon level. This result also led us to reexamine the lethality of the obliquely angled lesions as well. Thus, we have completed only the front-back paradigm at the 5% and 10% injury levels and the side to side paradigm at all three levels. As we have had to refine the balloon probe and overcome numerous developmental obstacles, we have not been able to complete a comprehensive anatomical analysis of the injury, including TUNEL staining.

Behavioral Testing

Rats surviving the trauma were tested at 1 hr, 24 hr, 48, hr, and 72 hr, post-injury. The scoring is done by two blinded observers. Three scales were used: The Neurological Severity Score (NSS), the Neurobehavioral Scale (NBS) and the NIH Stroke Severity Score (NIH).(Hallenbeck, Dutka et al. 1988)

The NSS was developed in 1988 (Shapira, Shohami et al. 1988), and is a widely used scale in which high scores indicate severe impairment and low scores indicate slight impairment or a normal rat. The maximum score on the NSS is 24. The NSS is scored either 1 (unable) or 0 (able) and examines the ability of the rat to perform in the following tasks. 1) Exit from a circle 50 cm in diameter. The rat is placed at the center of the circle and is given a point if unable to leave before 30 min, another point if it still is unable to leave before 60 min, and a point if unable to leave after 60 min. The first two time intervals of the circle test are only used at the 1 hr test.(Shohami, Novikov et al. 1995) The > 60 min interval continues to be used in the later tests. 2) Righting reflex. A normal rat instinctively rights itself when it is turned over. The recovering

rat is lying on its left (paretic) side. A point is assigned if the rat is unable to right itself 20, 40 and/or greater than 60 min after injury. The first two time intervals are only used at the 1 hr test. The last interval is still used in later tests. 3) Hemiplegia. The rat is pushed back and forth at the shoulders and should resist equally in both directions. A point is given if resistance is not equal. 4) Hind limb flexion. A normal rat when raised by the tail will extend both hind limbs, reaching upwards. If the rat flexes a hind limb, a point is given. 5) Walk in a straight line and ability to move. A point is allotted for each function. 6) Startle reflex to a loud noise about 20 cm above the rat's head. (Germano, Dixon et al. 1994) The rat should flinch heavily. If it does not, a point is given. 7) Pinna reflex to touching the external auditory meatus with a cotton tipped ear swab. (Chen, Li et al. 2001) If the rat does not shake its head back and forth, a point is assigned. 8) Seeking behavior and ability to stand. If a rat has lost its seeking behavior (a normal rat will walk around and sniff unknown objects), the rat receives a point. The point is only given if the rat would have been graded a 2 (moderate impairment) or lower on the corresponding category of the NBS. If the rat is prostrated, another point is given. 9) Placing reflexes. The rat is lifted 5 cm off the ground by the tail and back. The animal should "reach" for the ground and place its limbs on the floor with palms facing the ground. A point is allotted for each limb's inability to place. 10) Balance beam and beam walking. The rat is placed on a 1.5 cm wide beam. A point is given if the rat falls off within 60 sec, another point if that fall was within 40 sec, and another point if that fall was within 20 sec. The rat is then placed on beams 2.5 cm, 5.0 cm, or 8.0 cm in width. A point is given for failure on any width.

The NBS is divided into four categories. Rats are graded on a scale of 0-4, with 4 being normal and 0 being non-functional. The first category is forelimb flexion upon suspension by tail. A normal rat will extend both forelimbs and reach for the ground. (Bederson, Pitts et al. 1986) A "4" is given for normal forelimb extension, a "3" for slight forelimb flexion, a "2" for moderate forelimb flexion, a "1" for severe forelimb flexion, and a "0" if the forelimbs are tucked in next to the body. The second category is decrease in resistance to lateral pulsion. The rat is pulled by each limb. Resistance should be equal in both directions. A "4" is given for normal a "3" for slight impairment, a "2" for moderate impairment, a "1" for severe impairment, and a "0" for no resistance at all. The third category is circling behavior upon spontaneous ambulation. A normal rat, when placed on the floor should be able to walk straight. If the rat is able to walk straight even if it does show partial circling, it is given a "4". If the rat always walks to the paretic side, it is given a "3". If the rat shows partial circling and always walks to the paretic side, it is given a "2". If the rat circles when attempting to walk, it is given a "1". If the rat can only spin in place, it is given a "0". (Reglodi, Somogyvari-Vigh et al. 2000) The fourth category is ability to stand on an inclined plane. The rat is placed on an 8.0 cm wide board at a specified angle. The rat is given a "4" if it can stand on the 45°-50° board, a "3" if it can stand on a 40°-45° board, a "2" if it can stand on a 35°-40° board, a "1" if it can stand on a 30°-35° board, and a "0" if it cannot stand on the 30° board. The final category of the NBS is open-field activity/ exploratory behavior. The rat is placed on the floor and observed. A normal rat should explore the area and sniff unknown objects. A normally exploring rat is given a score of "4". A rat that sniffs and explores, but not to a normal degree, a "3" is given. If the rat either does not sniff or does not explore at all, a "2" is given. If the rat neither sniffs nor explores a "1" is given. If the rat does not move, a "0" is given.

The final scale is the NIH scale. A grade of 0 is given to a normal rat. A grade of 1 is given to a lethargic rat. A grade of 2 is given to a rat with clear signs of paresis, but with the ability to walk. A grade of 3 is given to a rat with the inability to walk. A grade of 4 is given to a dead rat. (Hallenbeck, Dutka et al. 1988)

Pathology

Following neurological testing on day 3, rats were perfused transcardially with 0.1M PBS followed by 10% formalin solution. Brains were removed from the cranium and embedded into paraffin. Coronal (medial-lateral) and sagittal (rostral-caudal) sections were cut on a microtome, deparaffinized and stained with either hematoxylin and eosin, or 0.5% cresyl violet solution. Sections were coverslipped and observed using a microscope. Cells were counted in 3 separate high power fields along the probe track (injured group) or at similar anatomical sites (sham group) by 2 different observers blinded to the animal's treatment. The mean of both observers and the 3 fields was recorded. Similar cell analysis was performed in the hippocampus ipsilateral to the probe track (injured group) or at a similar anatomical site (sham group).

Statistical Analysis

A Kruskal-Wallis One Way ANOVA on Ranks test with Tukey or Dunn's post-hoc analysis was performed on all behaviorally scored data.

Results

Survival following PTBI

Survival of animals subjected to sham, O-F and left-right operations are summarized in Table I. All of the sham-operated animals survived the surgery and the subsequent behavioral testing procedures, while several animals in either the O-F and left-right PTBI groups died following surgery.

Table I: Survival of Rats Following Penetrating Traumatic Brain Injury

<u>Group</u>	<u>Occipital-Frontal</u>	<u>Left-Right</u>
Sham	100%	100%
0% Balloon (injury)	100%	100%
5% Balloon (injury)	100%	91%
10% Balloon (injury)	62%	91%
15% Balloon (injury)	30%	71%

Increasing balloon size resulted in the increased number of deaths, especially in the O-F group, where there was a substantial increase in fatalities when the balloon size was doubled from 5% to 10%. Doubling the volume implies more energy is dissipated into the brain to produce a 5 to 10 % increase in the damage volume, but energy is not a linear function of the volumetric size. Since increasing the balloon size in the O-F group to 10%, resulted in a near 50% survival rate, we chose not to increase the balloon size to 15%. The survival rates suggest that injury size is not the only determinant in life or death outcomes, but more importantly, the trajectory or route of the injury.

Behavioral Testing

Animals surviving surgery were functionally examined using three different neurological tests. Sham-operated control and probe only (no balloon) animals exhibited little/no functional deficits as a result of O-F surgical procedures on the NSS, NIH and NBS behavioral tests, while 5% and 10% balloon groups exhibited significant ($p < 0.05$) behavioral deficits when tested 1 hr following surgery on all of these tests. The 5% and 10% PTBI animals were also impaired at the latter time points tested and did not recover to control levels prior to sacrifice (Figure 1). Specific tasks in which the PTBI animals had performed poorly included, walking in a straight line where lesioned animals walked in circles, forepaw and hindlimb flexion on the side opposite the lesion when lifted by the tail, and hemiplegia towards the side opposite the lesion.

Left-right PTBI animals exhibited significant neurological deficits ($p < 0.05$) one hour following injury. The NSS, NIH and NBS test results showed significant differences between the sham group and the 10% and 15% balloon groups one hour after injury. Moreover, the 15% group was significantly impaired on the NSS when tested 48 hrs after injury (Figure 2). As with the O-F lesioned groups, the left-right animals continued to show impairment on all neurological tests up to three days post-injury with some degree of recovery, but never to control levels. In contrast to the O-F group, animals in the left-right groups preferentially showed disturbances in balance and bilateral forepaw flexion when lifted by the tail.

Left-right lesioned animals scored higher (performed poorly) on the NSS tests and were better performers on the NBS tests in contrast to their O-F lesioned counterparts, that performed poorly on the NBS and scored lower (performed better) on the NSS tests. Since the NSS test is designed to assess reflexes and basic motor skills, poor performance on this test suggests bilateral damage to the reflex centers of the brain, which would abolish and/or diminish the reflex. On the other hand, O-F lesioned animals experienced difficulty in behavioral tasks such as movement and posture which suggests damage limited to one side of the brain. Moreover, increase in balloon size resulted in decreased performance in the behavioral tasks tested in both left-right and O-F groups, which support the survival data.

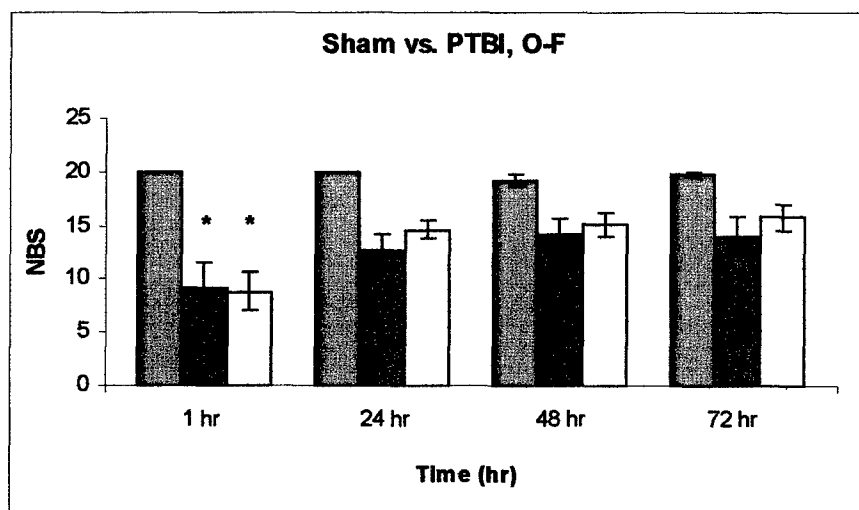
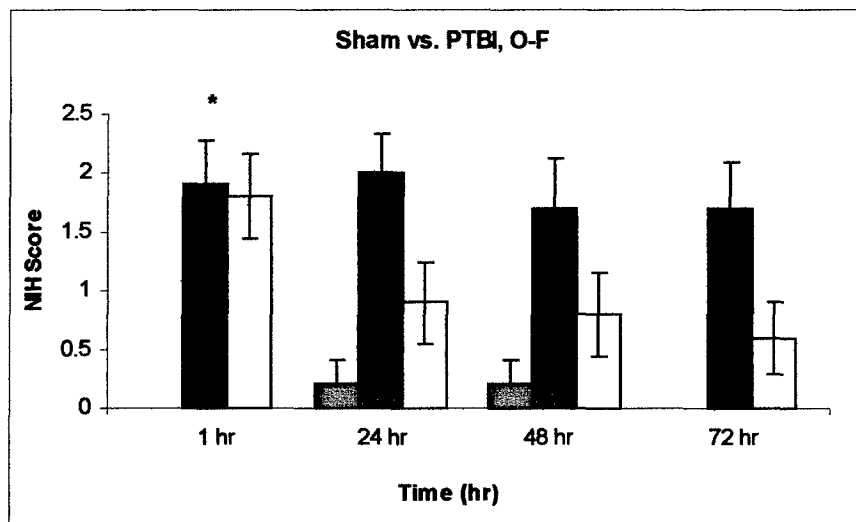
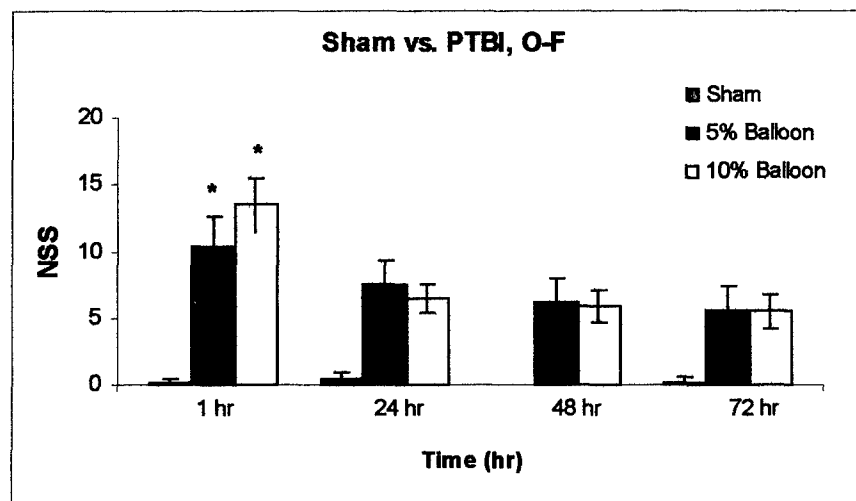


Figure 1. Effect of occipital-frontal lesions on the NSS, NIH and NBS behavioral assessments. Sham-operated animals suffered little/no functional deficits compared with 5% and 10% balloon PTBI animals.

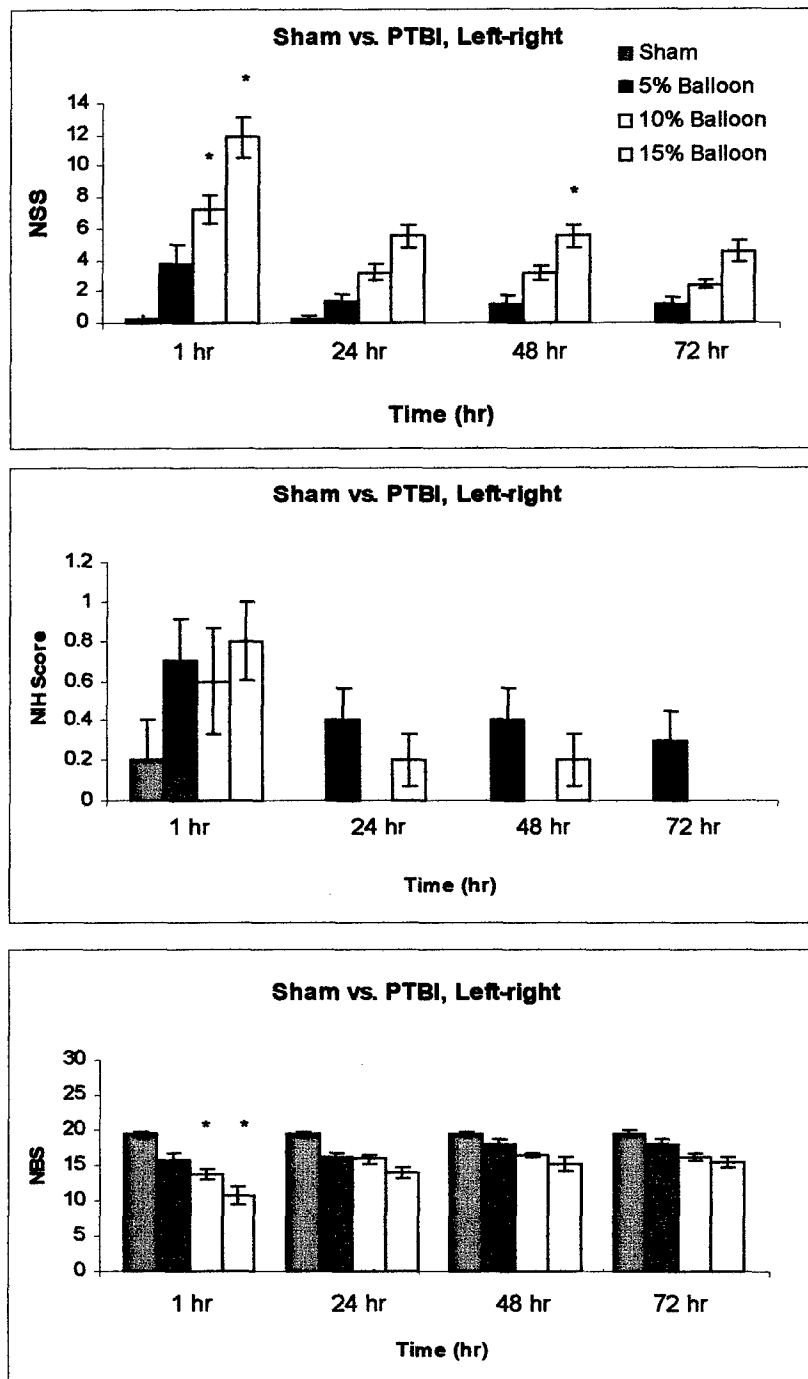


Figure 2. NSS, NIH and NBS behavioral test results from sham-operated and 5%, 10% and 15% left-right-lesioned animals. Sham-operated animals exhibited little/no behavioral deficits upon testing, while the lesioned animals exhibited neurological deficits.

Histopathology

Hematoxylin and eosin (H&E), and cresyl violet-stained sections of brains from PTBI animals revealed extensive neuronal death and gliosis in O-F and left-right sections. Examples of left-right lesions are depicted in Figures 3 and 4. Examples are from 10% balloon PTBI animals.



Figure 3 Hematoxylin and eosin-stained sagittal section of a left-right 10% balloon PTBI animal. Arrows point to the lesion created by the balloon.



Figure 4 High power magnification of lesion site. Black arrows delineate the outermost extent of the lesion (penumbral), while the white arrowheads mark the central area of the lesion occupied by the pale scar.

Examples of occipital-frontal lesions are depicted in Figure 5. Examples are from 10% balloon PTBI animals. Cell counts of the sham-operated and probe only (0% balloon) groups are depicted in Figure 6 for necrosis and Figure 7 for apoptosis (as measured using TUNL staining).

Occipital-frontal lesioned animals exhibited extensive damage on H&E stained sagittal brain sections with enlarged ventricles (Figure 5), which were not observed in left-right lesioned animals. The enlarged ventricle suggests increased cellular loss and/or damage, which could explain the behavioral and/or survival results.



Figure 5 O-F 10% PTBI lesioned animal. Arrows point to the lateral ventricle. Note the difference in the size of the lateral ventricle in the O-F lesioned animal when compared with the 10% left-right lesioned animal (Figure 3).

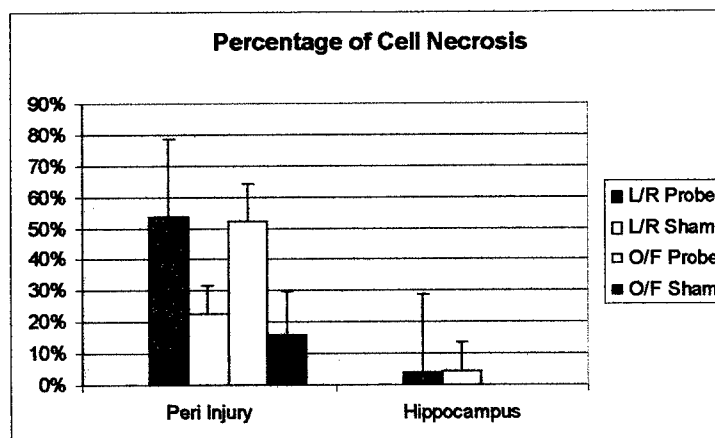


Figure 6. Cellular necrosis in peri-injury site and ipsilateral hippocampus. Probe with 0% balloon demonstrated significantly greater cellular injury than sham-operated animals. There was virtually no injury to hippocampus.

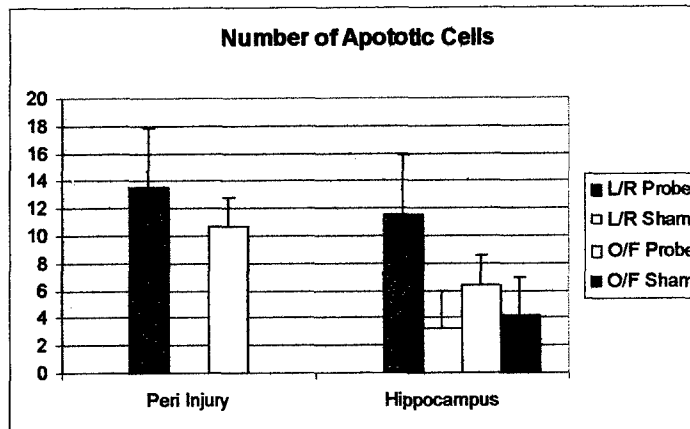


Figure 7. Apoptosis in peri-injury site and ipsilateral hippocampus. Probe with 0% balloon demonstrated significantly greater apoptotic cell damage than sham-operated animals. Although there was injury to the hippocampus, this was no significantly different from sham-operated animals.

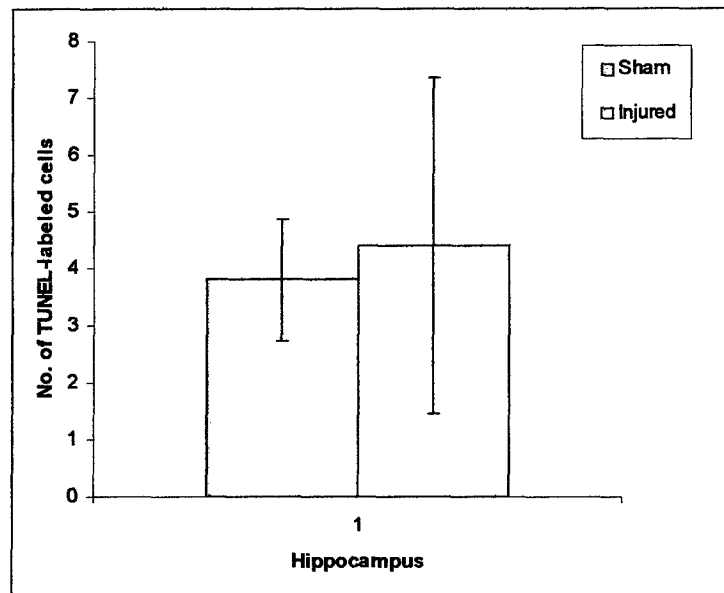
Insertion of probe, even without balloon inflation, resulted in significant cellular necrosis and apoptosis in peri-injury site along the probe track. However, there was little damage noted in ipsilateral hippocampus which is anatomically remote from this injury path.(Figs. 6 & 7)

TUNEL labelling of balloon in injured animals

In order to determine the extent of apoptosis or programmed cell death following PTBI, we labeled apoptotic cells using the TUNEL method. Examples of typical results are shown in Figure 6. TUNEL-labeled cells were most frequently observed at the entry of the probe and at the end of the probe (exit), but not at the dorsal or ventral boundaries of the lesion. Few labeled cells were observed in structures like the hippocampal formation, which on gross pathological examination, was not affected by the lesion in the side to side trajectory, as it was posterior to the probe. On the other hand, the cerebellum exhibited numerous labeled cells on back to front lesions, as the probe entered the brain through this structure.

Preliminary cell counts of TUNEL-labeled cells were conducted on the dorsal hippocampus on viable sections of 10% front-back lesioned animals (the left-right lesions damaged the dorsal hippocampus where counts were conducted, so no counts were obtained). Results are summarized in Figure 6. There was no statistically significant changes between sham-operated and injured animals in the number of TUNEL-labeled cells (n=5), suggesting that damage produced by the probe passing through the fimbria-fornix (see Figure 5) did not injure the dorsal hippocampus, at least after 3 days of survival.

Recently, studies have shown that the methodology used in the TUNEL labeling may be non-specific as it also labels dividing cells (Pulkkanen et al., 2000), necrotic cells (Garrity et al., 2003), as well as exhibiting false positive staining in response to proteinase K treatment (Stahelin et al., 1998) and histological sectioning (Sloop et al., 1999), the latter two methods having been used in our studies. To rectify the situation, we are currently employing immunohistochemical techniques to identify apoptotic cells using antibodies to cleaved caspase - 3 (Brecht et al., 2001).



DAPI

TUNEL

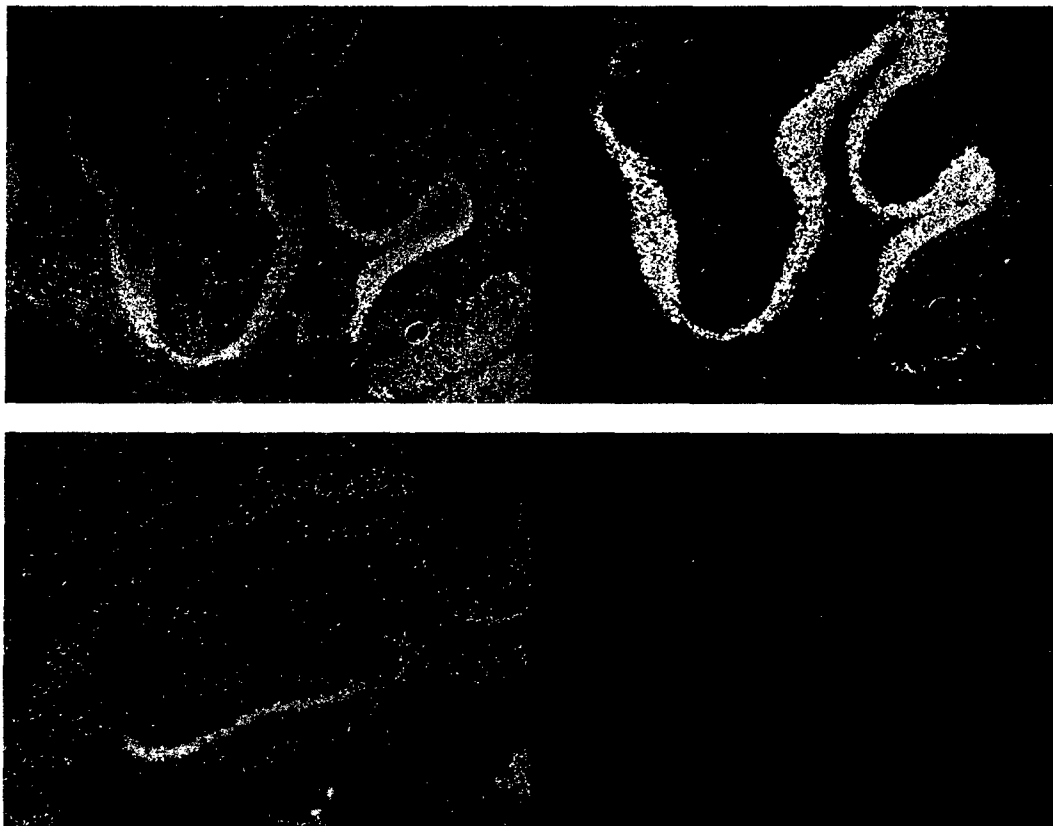


Figure 6. Photomicrographs of DAPI (nuclear) and TUNEL (apoptotic) cells in the cerebellum (upper panel) and hippocampus (lower panel) of PTBI brains.

To summarize, the two different PTBI models (left-right and occipital-frontal) produces extensive neuronal damage to the brains of rodents resulting in decreased survival, with each type of injury producing unique functional deficits. Histological examination of brains reveals gliosis and scar tissue formation at the site of the lesion with alterations in ventricular size, suggesting neuronal death and/or injury. These results support and validate the air-inflation model of PTBI as a "tool" by which one can examine the role of penetrating objects on neuronal integrity and the ensuing functional outcome following brain injury.

Key Research Accomplishments

The mathematical model is complete and maybe used as intended, to predict the size and shape of the temporary cavities for different impact energies and velocities associated with the 7.62 NATO round. This mathematical model is the first in the investigation of PTBI.

The mechanical model has been calibrated and used laboratory in vivo studies. The in vivo studies will serve to validate the mathematical / mechanical predictions.

The in vivo studies provide the data which validates this model and its use as a PTBI tool by which one can examine the role of penetrating objects on neuronal integrity and the ensuing functional outcome following brain injury.

Reportable Outcomes

Included are sample outcomes of the mathematical PTBI model. Based on these outcomes the mechanical probe was designed and in vivo studies were conducted on the rat specifically using the 7.62 NATO round. For other laboratory animals the mathematical will have to be re-scaled for the different animals and a new probe will have to be developed to be representative of the specific ammunition used.

Sample calculations for the 9mm predicting volume size and shape at various ranges:

9mm						
INPUTS						
mass (g)=	8	8	8	8	8	8
Muzzle velocity (m/s) (Vo)=	350	350	350	350	350	350
Muzzle energy(joules) (Eo)=	490	490	490	490	490	490
Range to target(m) (Rm)=	10	20	65	88	113	150
Coupling Coefficient Ka Ka=	0.43	0.43	0.43	0.43	0.43	0.43
Diameter (caliber) (cm) =	0.9	0.9	0.9	0.9	0.9	0.9
Vel/Range Coef . Br : Br=	0.68	0.68	0.68	0.68	0.68	0.68
Assumptions						
Energy Diss on Impact Eb (j) Eb=	127.8	127.8	127.8	127.8	127.8	127.8
Density of (gelatine/air) =	848	848	848	848	848	848
Dissipation into Temp Cav K3.=	0.83	0.83	0.83	0.83	0.83	0.83

*Dissipation time(sec) TM=	0.000411	0.000411	0.000411	0.000411	0.000411	0.000411
**Dissipation time(Sec) TM2=	0.000488	0.000488	0.000488	0.000488	0.000488	0.000488
Computing Energy & Velocities						
Energies						
Energy at range (j) E1 =	471.14496	452.6598	374.0546	336.7713	298.4655	246.016
Energy Diss in Free Flt EA (j) Ea=	18.85504	37.34016	115.9454	153.2287	191.5345	243.984
Energy Diss on Impact Eb (j) Eb=	127.8	127.8	127.8	127.8	127.8	127.8
Energy Avail at medium Ei (j) Ei=	343.34496	324.8598	246.2546	208.9713	170.6655	118.216
Energy Diss Stable Ec (j) Ec=	93.88422	91.11779	78.36407	71.59893	63.98435	51.99751
Energy avail for lg Cavity E2 (j) E2=	249.46074	233.7421	167.8905	137.3724	106.6812	66.21849
Energy Dissin lg cavity Ed (j) Ed=	207.052414	194.0059	139.3491	114.0191	88.54539	54.96135
Residual Er (joules) Er=	42.4083258	39.73615	28.54138	23.3533	18.1358	11.25714
Velocities						
Vel at range V1 (m/s) V1=	343.2	336.4	305.8	290.16	273.16	248
Computing V i (m/s) Vi=	292.978224	284.9824	248.1202	228.5669	206.5584	171.9128
Computing V 2 (m/s) V2 =	249.730224	241.7344	204.8722	185.3189	163.3104	128.6648
Computing Vc (m/s) Vc=	153.20266	150.9286	139.9679	133.7899	126.4756	114.0148
Computing Vd (m/s) Vd=	227.515062	220.2305	186.6475	168.8335	148.7829	117.2192
Computing Vr (m/s) Vr =	102.966409	99.66964	84.47098	76.40894	76.40894	67.33462
Dimensions-Low Speed						
Computing Vt1(m/s) Vt1=	89.8747633	86.99716	73.73093	66.69394	58.77337	46.30483
Computing Vt2(m/s) Vt2=	209.011077	202.319	171.4673	155.1022	136.6823	107.6857
Computing D1(cm) D1=	7.4762898	7.365316	6.830434	6.528946	6.172011	5.563923
Computing R1(cm) R1=	3.69385277	3.575583	3.030341	2.741121	2.415585	1.903129
Computing R2 (cm) R2=	8.59035528	8.31531	7.047305	6.3747	5.617641	4.42588
Volume lg temp (cm3) Vt Vt=	491.038117	445.3661	271.1134	200.6601	137.3231	67.15538
Volume Stable Cavity Vca Vca=	146.815641	144.6364	134.1326	128.2122	121.2029	109.2615
Total Volumes Vt + Vca(cm3)=	637.853758	590.0025	405.2461	328.8723	258.526	176.4169
Tot RAT Volume (cm3) Vrat=	0.94848142	0.907696	0.623456	0.505957	0.397732	0.271411
Rat Vol from Vt/672.5(cm3)Vrat1=	0.7301682	0.662254	0.403143	0.298379	0.204198	0.099859
Compute Rat Rr2(cm) Rr2=	0.68266728	0.66081	0.560043	0.506591	0.446428	0.35172
Compute Rat Rr1(cm) Rr1=	0.29354693	0.284148	0.240818	0.217834	0.191964	0.15124
Ref Volume lg temp (Vt) / 1345=	0.3650841	0.331127	0.201571	0.14919	0.102099	0.04993
Reference Total Volume/1345	0.47424071	0.438664	0.301298	0.244515	0.192213	0.131165
Reference Volume =Vt/1345	0.3650841	0.331127	0.201571	0.14919	0.102099	0.04993
Reference Volume Rat	0.3650841	0.331127	0.201571	0.14919	0.102099	0.04993

Sample calculations for the 7.62 NATO predicting volume size and shape at various ranges:

7.62 NATO						
INPUTS						
mass (g)=	9.5	9.5	9.5	9.5	9.5	9.5
Muzzle velocity (m/s) (Vo)=	830	830	830	830	830	830
Muzzle energy(joules) (Eo)=	3272	3272	3272	3272	3272	3272
Range to target(m) (Rm)=	25	50	619	648	684	734
Coupling Coefficient Ka Ka=	0.61	0.61	0.61	0.61	0.61	0.61
Diameter (caliber) (cm) =	0.78	0.78	0.78	0.78	0.78	0.78
Vel/Range Coef . Br : Br=	0.72	0.72	0.72	0.72	0.72	0.72
Assumptions:						
Density of (gelatine/air) =	848	848	848	848	848	848
Dissipation into Temp Cav K3.=	0.83	0.83	0.83	0.83	0.83	0.83
*Dissipation time(sec) TM=	0.00028	0.00028	0.00028	0.00028	0.00028	0.00028
**Dissipation time(Sec) TM2=	0.000406	0.000406	0.000406	0.000406	0.0004059	0.000406
Computing Energy & Velocities						
Energies						
Energy at range (j) E1 =	3131.884	2994.571	701.5838	627.421	541.11881	431.843
Energy Diss in Free Flt EA (j) Ea=	140.116	277.429	2570.416	2644.579	2730.8812	2840.157
Energy Diss on Impact Eb (j) Eb=	127.8	127.8	127.8	127.8	127.8	127.8
Energy Avail at medium Ei (j) Ei=	3004.084	2866.771	573.7838	499.621	413.31881	304.043
Energy Diss Stable Ec (j) Ec=	652.0733	636.075	262.5509	242.3326	216.80742	180.281
Energy avail for Ig Cavity E2 (j) E2=	2352.011	2230.696	311.2329	257.2884	196.5114	123.762
Energy Dissin Ig cavity Ed (j) Ed=	1952.169	1851.478	258.3233	213.5494	163.10446	102.7224
Residual Er (joules) Er=	399.8418	379.2183	52.90959	43.73903	33.406937	21.03954
Velocities						
Vel at range V1 (m/s) V1=	812	794	384.32	363.44	337.52	301.52
Computing V i (m/s) Vi =	795.2602	776.8724	347.5581	324.3199	294.98218	253.0001
Computing V 2 (m/s) V2 =	703.6762	685.2884	255.9741	232.7359	203.39818	161.4161
Computing Vc (m/s) Vc=	370.5112	365.9379	235.104	225.8703	213.64379	194.8176
Computing Vd (m/s) Vd=	641.0795	624.3275	233.2035	212.0325	185.30456	147.0571
Computing Vr (m/s) Vr =	290.1331	282.5516	105.5408	95.95945	83.863219	66.55356
Dimensions-Supersonic						
Computing Vt1(m/s) Vt1=	333.848	325.1243	121.4428	110.4179	96.499056	76.58132
Computing Vt2(m/s) Vt2=	547.2919	532.9906	199.0866	181.0129	158.19517	125.5431
Computing D1(cm) D1=	15.03905	14.85342	9.542871	9.168075	8.6718013	7.907646
Computing R1(cm) R1=	9.347745	9.103479	3.4004	3.0917	2.7019736	2.144277
Computing R2 (cm) R2=	15.32417	14.92374	5.574426	5.06836	4.4294649	3.515208
Volume Ig temp(cm3) Vt Vt=	5609.649	5181.283	270.0256	202.9584	135.47475	67.71076
Volume Stable Cavity Vca Vca=	295.3294	291.684	187.3981	180.0381	170.2925	155.2864
Total Volumes Vt + Vca(cm3)=	5904.979	5472.967	457.4238	382.9965	305.76725	222.9972
Tot RAT Volume (cm3) Vrat=	8.780637	8.138241	0.680184	0.569512	0.4546725	0.331594
Rat Vol from Vt/ 672.5(cm3)Vrat1=	8.341486	7.70451	0.401525	0.301797	0.2014494	0.100685
Compute Rat Rr2(cm) Rr2=	1.94114	1.890416	0.706122	0.642018	0.5610881	0.445278

EMTech Consultants, Inc. Proprietary Information

Compute Rat Rr1(cm) Rr1=	1.184095	1.153154	0.430735	0.391631	0.3422637	0.271619
Reference Total Volume/1345	4.390319	4.069121	0.340092	0.284756	0.2273362	0.165797
Reference Volume =Vt/1345	4.170743	3.852255	0.200763	0.150898	0.1007247	0.050343
Reference Volume Rat	4.170743	3.852255	0.200763	0.150898	0.1007247	0.050343

Conclusions- All objectives of this study have been met. To reiterate these objectives:

The initial objective is to develop a mathematical model for rats that describes the biophysics of wound formation following a ballistic injury. The bullet-size model will be the full metal jacket ammunition like the 7.62mm round and the 9mm which are most commonly used in the military. These equations can then be used generically to determine the dimensions of the salient features of ballistic injury, i.e. the size and shape of the permanent and temporary wound cavities, rapidity of expansion and duration of inflation. This is completed and sample results provided

The second objective is to develop a device for minimal invasive recreation of the wound in rats. This device will be based on an air inflation technique. It will be built exactly to precise specifications based on the above mathematical model. This device will be designed in accordance with all elements of the wound arising from a gunshot. The wound cavities assume the proper size, shape and for the appropriate duration. This is completed and specifically developed for the 7.62 NATO round appropriate for the laboratory rat.

The third objective will be to conduct in vivo validation study in rats to demonstrate that this model can recreate wounds similar to those caused by military gunshot. Histopathologic findings will be compared to the results from human gunshot victim autopsy reports and to the work of Carey et al (1989, 1990) using the now-abandoned fired projectile feline model. This has been completed and the in vivo studies support and validate the air-inflation model of PTBI as a "tool" by which one can examine the role of penetrating objects on neuronal integrity and the ensuing functional outcome following brain injury

References

- 1) Carey, M. E., Sarna, G. S., Farrell, J. B. "Brain edema following an experimental missile wound to the brain" *J. Neurotrauma* 7: 13-20 (1990)
- 2) Carey, M.E, Sarna, G. S., Farrell, J. B., Happel, L. T. "Experimental missile wound to the brain" *J. Neurosurgery* 71:754-764 (1989)
- 3) Sellier and B.P. Kneubuehl, "Wound Ballistics and the Scientific Background", 1994 Chapter 4, Ammunition and Arms, Ballistics, Pages 111 to 123.
- 4) R. Bellamy and R. Zajtcuk, "The Text Book of Military Medicine, Part1, Volume 5", 1998, Chapter 4, Pages 107 -144.
- 5) W.J.Bruchey, "Ammunition for Law Enforcement: Part I, Methodology for evaluating relative stopping power and results", Technical Report ARBRL-TR-02199, October 1979.
- 6) W.J.Bruchey, B. Izdebski, H. Offney, B. Rickter, J. Haynie, "Ammunition for Law Enforcement: Part II, Data Obtained for Bullets Penetrating Tissue Simulant", Report number 1940, October 1976.
- 7) W.J.Bruchey, B. Izdebski, H. Offney, B. Rickter, J. Haynie, "Ammunition for Law Enforcement: Part III, Photographs of Bullets Recovered After Impacting Tissue Simulant", Report number 1940, October 1976.
- 8) Walker, Alan and Shipman, Pat "The wisdom of the bones" New York Knopf, 1996
- 9) Bederson, J. B., L. H. Pitts, et al. (1986). "Rat middle cerebral artery occlusion: evaluation of the model and development of a neurologic examination." *Stroke* 17(3): 472-6.
- 10) Chen, J., Y. Li, et al. (2001). "Therapeutic benefit of intravenous administration of bone marrow stromal cells after cerebral ischemia in rats." *Stroke* 32(4): 1005-11.
- 11) Germano, A. F., C. E. Dixon, et al. (1994). "Behavioral deficits following experimental subarachnoid hemorrhage in the rat." *J Neurotrauma* 11(3): 345-53.
- 12) Hallenbeck, J. M., A. J. Dutka, et al. (1988). "Stroke risk factors prepare rat brainstem tissues for modified local Shwartzman reaction." *Stroke* 19(7): 863-9.
- 13) Reglodi, D., A. Somogyvari-Vigh, et al. (2000). "Neuroprotective effects of PACAP38 in a rat model of transient focal ischemia under various experimental conditions." *Ann N Y Acad Sci* 921: 119-28.
- 14) Shapira, Y., E. Shohami, et al. (1988). "Experimental closed head injury in rats: mechanical, pathophysiologic, and neurologic properties." *Crit Care Med* 16(3): 258-65.

- 15) Shohami, E., M. Novikov, et al. (1995). "Long-term effect of HU-211, a novel non-competitive NMDA antagonist, on motor and memory functions after closed head injury in the rat." Brain Res **674**(1): 55-62.
- 16) Brecht S., Gelderblom M., Srinivasan A., Mielke K., Dityateva G., Herdegen T. (2001) Caspase-3 activation and DNA fragmentation in primary hippocampal neurons following glutamate excitotoxicity. Brain Res. Mol. Brain Res., 94(1-2):25:34.
- 17) Stahelin, B.J., Marti, U., Solioz M., Zimmermann H., Reichen J. (1998) False positive staining in the TUNEL assay to detect apoptosis in liver and intestine is caused by endogenous nucleases and inhibited by diethyl pyrocarbonate. Mol. Pathol. 51(4):204-208.
- 18) Sloop G.D., Roa J.C., Delgado A.G., Balart J.T., Hines M.O. 3rd, Hill J.M. (1999) Histologic sectioning produces TUNEL reactivity. A potential cause of false-positive staining. Arch. Pathol. Lab. Med., 123(6):529-532.
- 19) Garrity M.M., Burgart L.J., Riehle D.L., Hill E.M., Sebo T.J., Witzig T. (2003) Identifying and quantifying apoptosis: Navigating technical pitfalls. Modern Pathology, 16(4):389-394.
- 20) Pulkkanen K.J., Laukkanen M.O., Naarala J., Yia-Herttuala S. (2000) False-positive apoptosis signal in mouse kidney and liver detected with TUNEL assay. Apoptosis, 5:329-333.



DEPARTMENT OF THE ARMY
US ARMY MEDICAL RESEARCH AND MATERIEL COMMAND
504 SCOTT STREET
FORT DETRICK, MD 21702-5012

REPLY TO
ATTENTION

MCMR-ZC-I

29 Jun 04


MEMORANDUM FOR Administrator, Defense Technical Information
Center (DTIC-OA), 8725 John J. Kingman Road, Fort Belvoir,
VA 22060-6218

SUBJECT: Request Change in Distribution Statement

1. The U.S. Army Medical Research and Materiel Command has reexamined the need for the limitation assigned to technical reports written for Grant DAMD17-01-1-0742. Request the limited distribution statement for Accession Document Numbers ADB287012 and ADB292823 be changed to "Approved for public release; distribution unlimited." These reports should be released to the National Technical Information Service.

2. Point of contact for this request is Ms. Judy Pawlus at DSN 343-7322 or by e-mail at judy.pawlus@amedd.army.mil.

FOR THE COMMANDER:


PHYLIS M. RINEHART
Deputy Chief of Staff for
Information Management